engineering proceedings

Proceeding Paper

Buckling-Restrained Aluminum Shear-Yielding Dampers for RC Seismic Retrofit: Hysteretic Response and Structural Performance †

Osvaldo Pecorari [1], Euripidis Mistakidis [2], Massimiliano Ferraioli [1] and Alberto Mandara [1,*]

[1] Department of Engineering, University of Campania "Luigi Vanvitelli", 81031 Aversa, Italy; osvaldo.pecorari@unicampania.it (O.P.); massimiliano.ferraioli@unicampania.it (M.F.)
[2] Department of Civil Engineering, University of Thessaly, 38221 Volos, Greece; emistaki@o365.uth.gr
* Correspondence: alberto.mandara@unicampania.it; Tel.: +39-081-50-10216

† Presented at the 16th International Aluminium Conference (INALCO 2026), Trondheim, Norway, 10–12 June 2026.

Abstract

This study explores the use of buckling-restrained aluminum shear-yielding panels (BRASYPs) as energy-dissipation devices. These are integrated into exoskeletons designed for sustainable interventions. A retrofit strategy was defined for a school building employing exoskeletons integrating BRASYPs. A displacement-based retrofit strategy was applied and validated through nonlinear time-history analyses. Results confirm the effectiveness of the intervention: the peak inter-story drift ratio remains below the collapse-prevention limit, and devices dissipate energy according to design.

Keywords: shear-yielding aluminum dampers; seismic retrofit; RC buildings; exoskeletons

Academic Editor: Sigmund Arntsønn Tronvoll

Published: 15 July 2026

1. Introduction

In highly seismically active zones, buildings originally built without seismic considerations now frequently serve strategic purposes. Due to poor maintenance, continuous degradation, and inadequate structural monitoring, their seismic risk naturally rises with time. While maintaining linear and elastic behavior during earthquakes is the primary goal of typical retrofit procedures, this strategy can sometimes result in an unduly stiff retrofitted building, which may unintentionally increase seismic demands. The development and application of technologies intended to disperse seismic input energy has proven to be the most successful strategy [1]. When certain force thresholds are reached, passive seismic dampers disperse energy through stable plastic deformation, protecting structures during strong earthquakes. Because of their dependable energy dissipation, independence from loading rate, affordability, ease of production, and repositionability, metallic yielding dampers, which serve as passive energy-dissipation systems, are frequently chosen. They improve the structural strength, stiffness, and ductility of metal-plate shear walls [2]. The mechanical behavior and chemical composition of materials, particularly low-yield-strength steels, metal alloys, and aluminum, have been the subject of extensive investigation [3]. This work builds upon the previous study regarding the hysteretic behavior of buckling-restrained aluminum shear-yielding panels (BRASYPs) [4]. These dampers ensure steady energy dissipation while preventing premature buckling by leveraging aluminum's ductility. The displacement-based design approach was then used to design the BRASYPs as dissipative components in a seismic retrofit plan for a school in Grottaminarda, Italy. Dissipative eccentrically braced steel frames are used in this intervention. Nonlinear time-history studies are used to verify the design's efficacy. The performance of the retrofitted structure was verified using a set of ground movements scaled for the collapse-prevention limit state in accordance with the spectrum-compatibility standards of the Italian Building Code (2018) [5].

2. Behavior of Buckling-Restrained Aluminum-Based Shear-Yielding Panels

2.1. Shape-Optimization Strategy

Localizing the damage into components that are simple to produce, install, monitor, and maintain, the use of metallic plates as energy-dissipation devices has been successful in increasing structural resilience. In line with this strategy, many studies have focused on improving the form of these plates [6]. The overall dissipative capacity of standard rectangular designs is sometimes limited by stress concentrations at the corners. Alternatively, hourglass-shaped panels have been produced and compared with rectangular ones in compliance with the Von Mises yield requirement [7]. The hourglass-shaped aluminum-based shear-yielding panels (ASYPs) (Figure 1a) have a constant thickness (t). Hourglass shapes are characterized by a maximum width (h_p) and a minimum width ($h_{p,1}$) and height (b_p). The numerical analyses [4] are based on an increasing aspect ratio (AR = h_p/b_p) and utilize the mechanical properties of an Annealed Al-19000 alloy, characterized by a Young's modulus (E) of 35115 MPa, a yield strength (σ_y) of 33 MPa, an ultimate tensile strength (σ_u) of 75 MPa, and an ultimate elongation (ε) of 32% [8]. Although the Young's modulus value experimentally measured in [8] is atypically low, it does not have a significant impact on the panel's capacity for energy absorption. Such analysis and configuration demonstrated consistent hysteretic performance at low shear-strain values. Higher strains, however, caused out-of-plane buckling, which led to a discernible loss of strength in the hysteresis loops. A revised energy-dissipation system was implemented to mitigate this instability and provide a steady resistance. Stiff L-shaped steel profiles are intended to be elastic as inhibitors for the aluminum web plate, limiting out-of-plane deformation. The aluminum plate is positioned between two solid components, each 10 mm thick, in the finite element model of the buckling-restrained panel (Figure 1b), permitting unrestricted in-plane movement within a 6.6 mm clearance.

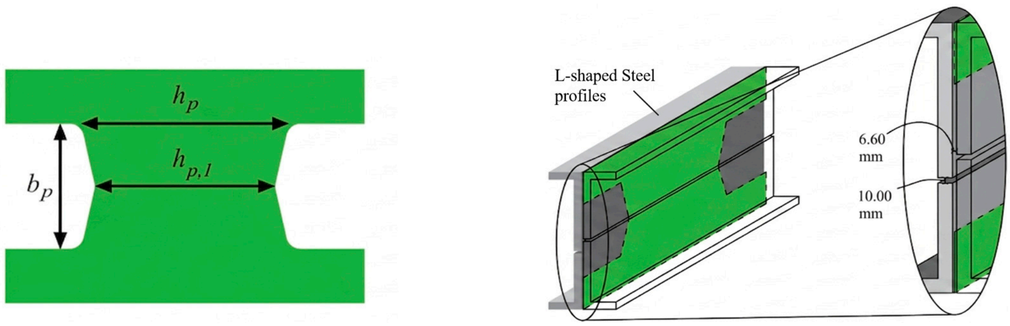

(**a**) (**b**)

Figure 1. (**a**) Geometric properties of the hourglass-shaped ASYP; (**b**) BRASYP model.

This configuration allows these devices to be utilized as dissipators through stable hysteretic cycles (Figure 2a). The hourglass shape facilitates full exploitation of the panel's yielding capacity without failure, ensuring a widespread distribution of Von Mises equivalent stress (Figure 2b) and equivalent plastic strain (Figure 2c) across the entire plate surface. This prevents localized stress concentrations at the corners.

https://doi.org/10.3390/engproc2026151002

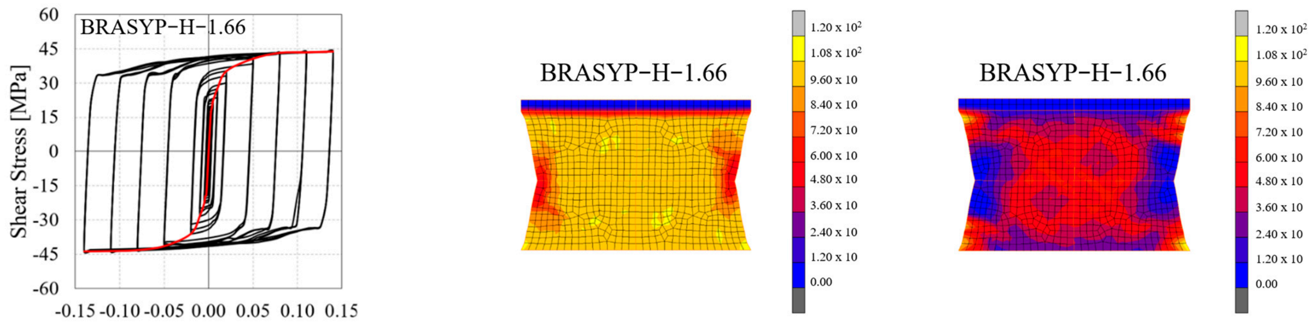

(**a**) (**b**) (**c**)

Figure 2. (**a**) BRASYP hysteretic loops; (**b**) Von Mises equivalent stress; (**c**) total equivalent plastic strain.

2.2. Definition of BRASYP's Equivalent Stiffness

To design these dampers in a practical retrofit scenario, it is essential to delineate the characteristics required for their sizing. The principle of virtual work is employed to analytically define the equivalent stiffness (K_e) [9]. The aluminum-based panel is represented as an equivalent beam with fixed ends (Figure 3). The equivalent stiffness is defined by the combination of the shear (Q_x) and the bending moment (M_x) computed relative to the distance from the center, x, as

$$1 \cdot \delta = \int_{-b_p/2}^{b_p/2} \frac{M_x m_x}{EI_x} dx + \int_{-b_p/2}^{b_p/2} \frac{Q_x q_x}{GA_x} dx. \tag{1}$$

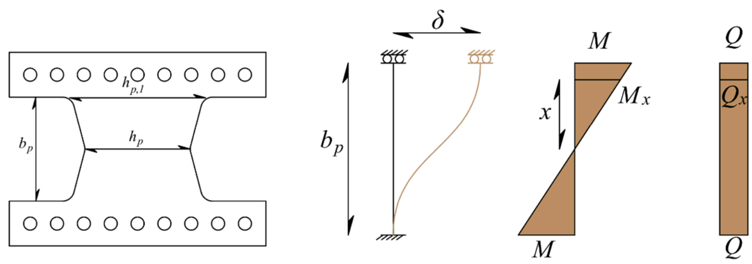

Figure 3. Equivalent beam with fixed ends subject to a unit displacement.

The top displacement of the lamina is denoted by δ. I_x indicates the moment of inertia of the section at a distance x from the centroid, E represents the Young's modulus of aluminum, G signifies the shear modulus of the material, and A_x indicates the cross-sectional area relative to the centroid x. The elastic stiffness of the BRASYP can be characterized as the ratio of the yielding shear (Q_y) over the yielding displacement (δ_y). In this paper, the shape of the dampers was checked to avoid any degradation.

$$K_e = \frac{Q_y}{\delta_y} \tag{2}$$

3. Seismic Retrofit of an RC School Building

The device was defined for the seismic retrofit of a reinforced concrete (RC) school building in Grottaminarda, Italy, in the 1980s. The building, which has three stories above ground and a basement, is situated on Type C soil (T1 topography) with shallow foundations (Figure 4). Extensive data collection is used to derive material attributes, yielding a KL2 knowledge level. For seismic verification, the mean material strength values

(f_{cm} = 24.54 MPa for concrete and f_{ym} = 385.3 MPa for steel) were used. Inelastic force-based fiber elements (infrmFBs) were used to model the case study in SeismoStruct 2025 [10]. Sections were discretized into steel, confined concrete [11], and unconfined concrete fibers. A bilinear hysteretic model was used to simulate the reinforcement. Eigenvalue and nonlinear (pushover) analyses were performed with 5% accidental eccentricity, taking into account modal (Group 1) and uniform (Group 2) force distributions. According to Eurocode 8 [12], the limit states of Immediate Occupancy (IO), Damage Limitation (DL), Life Safety (LS), and collapse prevention (CP) are defined. Chord rotation and shear strength are used to evaluate the capacity of brittle and ductile components, respectively. According to formula C.8.7.2.1 of the Italian Code Instructions (2019) [13], chord rotation characterizes the deformation capacity of beams and columns. The methodology described in both the Italian Code Instructions and Annex B of Eurocode 8 is used to evaluate capacity against demand for the LS limit state. Table 1 presents the synthesis of the seismic safety verification for each case study, illustrating the school building's safety index (ζ) regarding peak ground acceleration (PGA). Seismic retrofitting in the X-direction is required, according to the structure's seismic assessment. On the other hand, even at the collapse-prevention limit state, the structure is validated in the Y-direction. This is mostly because all of the columns' strong axes are oriented along the Y-axis.

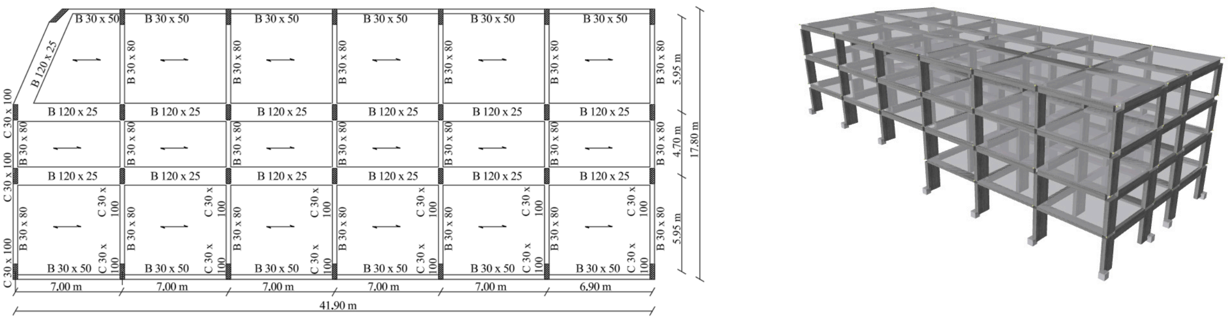

(**a**) (**b**)

Figure 4. (**a**) Plan view; (**b**) 3D view.

Table 1. Safety index (ζ) in terms of PGA.

	ζ(PGA)			
	IO	**DL**	**LS**	**CP**
X-Direction	0.577	0.572	0.603	0.753
Y-Direction	2.033	1.685	1.462	2.167

Parallel V-Shaped Dissipative Exoskeleton Design

V-shaped elastic steel exoskeletons are fitted with BRASYP devices. The installation of dampers in tandem with exoskeletons was evaluated using alternative technologies, such as flexural plates [14] or self-centering systems [15]. Significant energy absorption during numerous stable cycles and inelastic deformation is made possible by the aluminum alloy's improved ductility. As structural "fuses," these dampers concentrate seismic damage inside components that are easily accessible. By guaranteeing that panels can be efficiently inspected and replaced, this design enables the prompt restoration of building operations following a major earthquake while maintaining the integrity of the main structure. The displacement-based approach presented by Mazza and Vulcano [16] is used in the retrofit design. In particular, the process for sizing the dissipative exoskeletons with BRASYP dampers follows the established design procedure provided by Ferraioli et al. [17,18] for dissipative exoskeletons placed parallel to the façade of a building. The existing structure's equivalent single degree of freedom (SDOF) system (Table 2) is established from the lowest pushover curve (Figure 5). The target design displacement (d_p) is determined based on ductile failure modes, identifying the corresponding performance-based shear ($V_p^{(S)}$). Bilinear idealization per ATC-40 [19] provides key parameters: yield displacement ($d_y^{(S)}$), base shear ($V_y^{(S)}$), hardening ratio ($r^{(S)}$), and ductility ($\mu^{(S)}$). Equivalent viscous damping of the structure combines 5% structural damping ($\xi_v^{(S)}$) with equivalent viscous damping due to hysteresis ($\xi_h^{(S)}$). Similarly, the dissipative exoskeleton (E) is characterized as an SDOF system at d_p (Table 3). Since the initial stiffness and strength of the BRASYP dampers are unknown, the retrofitted building is modeled as a parallel system of the existing structure (S) and the exoskeleton (E). The combined hysteretic damping ($\xi_h^{(SE)}$) is calculated as a weighted mean of the base shear ratios of S and E. Finally, the effective period (T_e) and equivalent stiffness (K_e) of the retrofitted building are derived using the $\xi_h^{(SE)}$-damped spectral displacement at the target d_p. Since the exoskeleton's design base shear ($V_p^{(E)}$) and the combined hysteretic damping ($\xi_h^{(SE)}$) are initially unknown, an iterative design process is employed. The total design shear is distributed vertically based on the first mode shape, determining the required story strength ($V_{y,i}$) and stiffness (K_i) per frame (Table 4). Strength and stiffness are divided equally among seven parallel dissipative exoskeletons (BRSs) distributed in plan (Figure 6a). This results in the BRASYP's target strength ($Q_p^{\,t}$) and stiffness ($K_y^{\,t}$) at each story for every BRS (Table 5). Figure 6b illustrates the ultimate planar configuration of a single-span BRS.

Table 2. Parameters of bilinear SDOF system—as-built structure (S).

Dir.	m_e^*	Γ	d_p	d_p^*	$V_p^{(S)}$	$V_y^{(S)}$	$d_y^{(S)}$	$K_e^{(S)}$	$T_e^{(S)}$	$r^{(S)}$	$\mu^{(S)}$	$\xi_h^{(S)}$
	[kNs²/mm]	[-]	[mm]	[mm]	[kN]	[kN]	[mm]	[kN/mm]	[s]	[-]	[-]	[%]
X	1.280	1.313	99.0	73.4	2490	1163	9.20	25.15	1.417	0.12	10.8	0.13

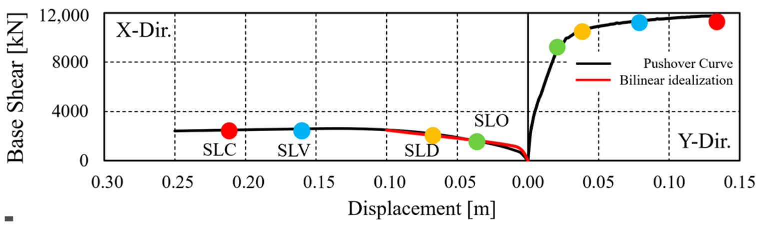

Figure 5. Pushover curve and bilinear idealization.

Table 3. Parameters of bilinear SDOF system—exoskeleton (E).

Dir.	d_p	d_p^*	$V_p^{(E)}$	$V_y^{(E)}$	$d_y^{(E)}$	$K_e^{(E)}$	$r^{(E)}$	$\mu^{(E)}$	$\xi_h^{(E)}$
	[mm]	[mm]	[kN]	[kN]	[mm]	[kN/mm]	[-]	[-]	[%]
X	99.0	73.4	970	490	0.62	7.90	0.13	79.0	0.31

Table 4. Strength and stiffness of the exoskeleton over the height.

Floor	M	Eigenvector	F_i	$V_{y,i}$	K_i	n_{BRS}
	[kNs²/mm]	[ϕ_1]	[kN]	[kN]	[kN/mm]	[-]
1	701.7	0.310	66	369.7	1177.0	7
2	694.2	0.730	153	303.9	483.8	7
3	498.9	1.00	151	150.8	373.4	7

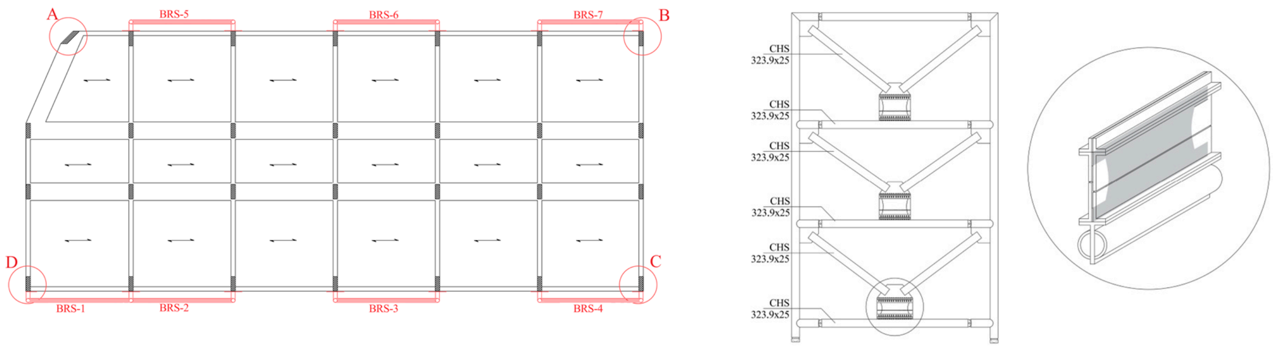

(**a**) (**b**)

Figure 6. (**a**) Layout in plan of the retrofitted structure; (**b**) detail of a single-span BRS.

Table 5. Properties of BRASYP dampers.

Floor	$Q_p{}^t$ [kN]	$K_y{}^t$ [kN/mm]	b_p [mm]	h_p [mm]	t [mm]	$h_{p,1}$ [mm]
1	52.8	85.2	350	970	3	924
2	43.4	58.2	560	870	3	760
3	21.5	24.9	560	517	3	376

4. Seismic Assessment

Nonlinear time-history analysis on a 3D model defined in SeismoStruct is used to assess the efficacy of the seismic intervention. The structure is simultaneously subjected to two-way horizontal ground motions. In order to ensure compliance with the spectrum-compatibility guidelines set forth by the Italian Code (2019) [13] and Eurocode 8 [12], these recordings were chosen and scaled using the REXEL computer code [20]. Figure 7 shows the relationship between the target spectrum and the average spectrum for the selected signals. The peak inter-story drift ratio (IDR) and maximum floor accelerations measured at the corner columns (A, B, C, and D) throughout the building's height for the collapse-prevention (CP) limit state are shown, respectively, in Figures 8 and 9. The IDR profiles show a consistent distribution across the height, with the second level showing the highest values. The performance requirements for collapse prevention are met since the highest IDR stays within the 2% transient drift threshold. Figure 10 depicts the hysteretic behavior of specific BRASYP dampers (i.e., BRS-3) at different floor levels. The retrofit approach and design are validated by the consistent yielding of all devices within the retrofitted structure.

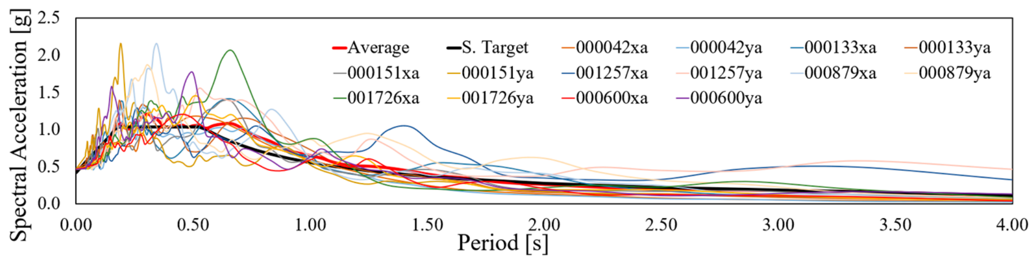

Figure 7. Earthquake records.

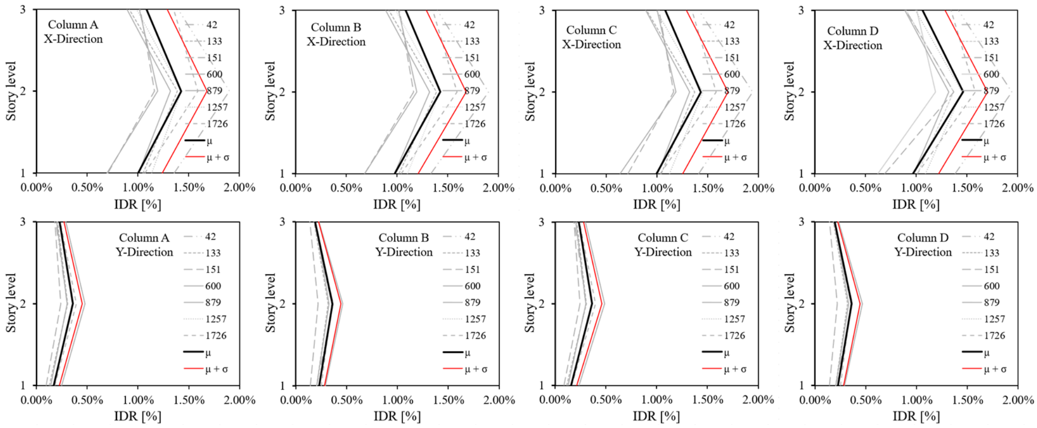

Figure 8. Peak inter-story drift ratio (IDR) over the height.

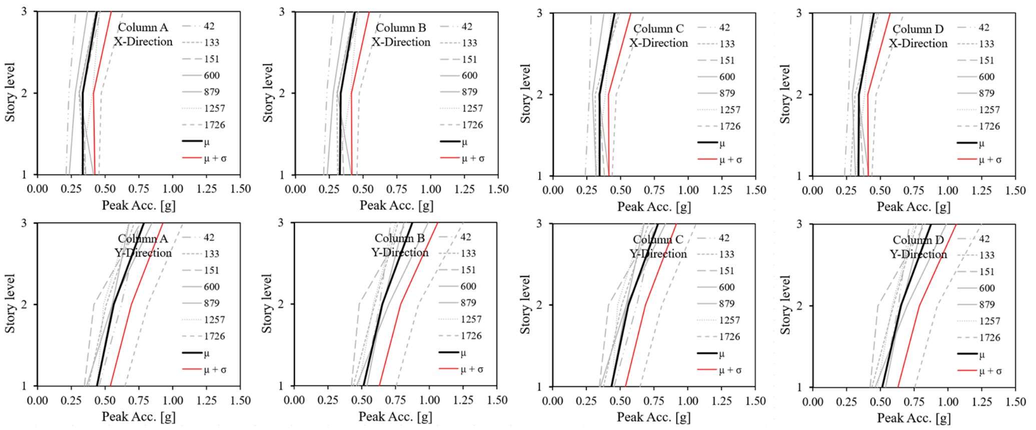

Figure 9. Peak absolute acceleration over the height.

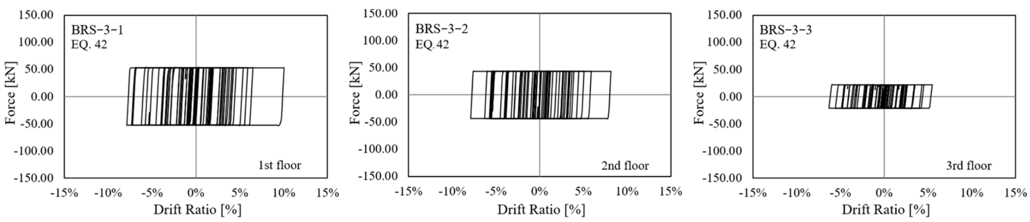

Figure 10. Hysteresis loops of BRASYP dampers.

5. Conclusions

This study assesses aluminum shear dampers with hourglass and rectangular shapes. A buckling-restrained model, which incorporates lateral steel plates to reduce instability without direct first contact, was developed as a result of the early ASYP designs' susceptibility to out-of-plane instability. Using dissipative eccentrically braced frames, these devices were designed using displacement-based design for the seismic retrofitting of a Grottaminarda school. Nonlinear time-history analyses validated the intervention in the critical X-direction. The average IDR was 1.48%, the mean peak floor acceleration was 0.52 g, and the dampers showed consistent yielding throughout the building's height, confirming the strategy's efficacy and guaranteeing strong energy dissipation and collapse avoidance.

Author Contributions: Conceptualization, O.P., M.F., E.M. and A.M.; methodology, O.P., E.M., M.F. and A.M.; software, O.P. and M.F.; validation, O.P., M.F. and E.M.; formal analysis, O.P. and M.F.; investigation, O.P., M.F. and E.M.; resources, E.M. and M.F.; data curation, O.P., E.M. and M.F.; writing—original draft preparation, O.P.; writing—review and editing, O.P., M.F., E.M. and A.M.;

visualization, O.P., M.F. and E.M.; supervision, E.M. and A.M.; project administration, O.P. and A.M. All authors have read and agreed to the published version of the manuscript.

Funding: The research activity is included in the ReLUIS-DPC 2024-2026 Research Project: WP5: "Integrated and Sustainable Interventions for Existing Buildings" funded by the Italian Department of Civil Protection (DPC).

Institutional Review Board Statement: Not applicable.

Informed Consent Statement: Not applicable.

Data Availability Statement: The data that supports the findings of this study are available from the corresponding author upon reasonable request.

Conflicts of Interest: The authors declare no conflicts of interest.

Abbreviations

The following abbreviations are used in this manuscript:

ASYP	Aluminum-based shear-yielding panel
BRASYP	Buckling-restrained aluminum-based shear-yielding panel
AR	Aspect ratio
RC	Reinforced concrete
IO	Immediate occupancy
DL	Damage limitation
LS	Life safety
CP	Collapse prevention
PGA	Peak ground acceleration
SDOF	Single degree of freedom
IDR	Inter-story drift ratio

References

1. Arvind, R.; Santhi, M. A state of art review on hybrid passive energy dissipating devices. *J. Vib. Eng. Technol.* **2022**, *10*, 1931–1954. [CrossRef]
2. Formisano, A.; Lombardi, L.; Mazzolani, F.M. Perforated metal shear panels as bracing devices of seismic-resistant structures. *J. Constr. Steel Res.* **2016**, *126*, 37–49. [CrossRef]
3. Brando, G.; De Matteis, G. Experimental and numerical analysis of a multi-stiffened pure aluminium shear panel. *Thin-Walled Struct.* **2011**, *49*, 1277–1287. [CrossRef]
4. Pecorari, O.; Mistakidis, E.; Ferraioli, M. Hysteretic behavior of buckling-restrained aluminum shear-yielding dampers. In Proceedings of the 10th International Conference on Computational Methods in Structural Dynamics and Earthquake Engineering, Rhodes Island, Greece, 15–18 June 2025. [CrossRef]
5. Ministry of Infrastructure and Transport. Update of the Technical Standards for Construction. (18A00716) (OJ General Series No.42 of 20-02-2018—Suppl. Ordinary No. 8). Available online: https://www.gazzettaufficiale.it/eli/id/2018/02/20/18A00716/sg (accessed on 10 July 2026).
6. Hu, J.W.; Cha, Y.W.; Farzampour, A.; Mirzai, N.M.; Mansouri, I. Experimental study on the optimized design of butterfly-shaped dampers. *Smart Struct. Syst.* **2021**, *27*, 795–801. [CrossRef]
7. Liu, Y.; Shimoda, M. Shape optimization of shear panel damper for improving the deformation ability under cyclic loading. *Struct. Mult. Opt.* **2013**, *48*, 427–435. [CrossRef]
8. Yadav, D.; Sahoo, D.R. Experimental and analytical investigations of buckling-inhibited aluminum shear yielding devices under cyclic loading. *Soil. Dyn. Earth. Eng.* **2023**, *172*, 108007. [CrossRef]
9. Li, Y.W.; Li, G.Q.; Sun, F.F.; Jiang, J. Experimental study on continuous energy-dissipative steel columns under cyclic loading. *J. Constr. Steel Res.* **2018**, *141*, 104–117. [CrossRef]
10. Seismosoft. SeismoStruct—A Computer Program for Static and Dynamic Nonlinear Analysis of Framed Structures. 2025. Available online: https://seismosoft.com (accessed on 10 July 2026).
11. Mander, J.B.; Priestley, M.J.; Park, R. Theoretical stress-strain model for confined concrete. *J. Struct. Eng.* **1988**, *114*, 1804–1826. [CrossRef]

12. *EN 1998-3*; Eurocode 8—Design of Structures for Earthquake Resistance—Part 3: Assessment and Retrofitting of Buildings. European Communities for Standardization: Brussels, Belgium, 2005.
13. Ministry of Infrastructure and Transport. Instructions for the application of the "Update" construction techniques referred to in Ministerial Decree 17 January 2018. (19A00855) (OJ General Series No. 35 of 11-02-2019—Suppl. Ordinary No. 5). Available online: https://www.gazzettaufficiale.it/eli/id/2019/02/11/19A00855/sg (accessed on 10 July 2026).
14. Eatherton, M.R.; Ma, X.; Krawinkler, H.; Mar, D.; Billington, S.; Hajjar, J.F.; Deierlein, G.G. Design concepts for controlled rocking of self-centering steel-braced frames. *J. Struct. Eng.* **2014**, *140*, 04014082. [CrossRef]
15. Lee, C.H.; Ju, Y.K.; Min, J.K.; Lho, S.H.; Kim, S.D. Non-uniform steel strip dampers subjected to cyclic loadings. *Eng. Struct.* **2015**, *99*, 192–204. [CrossRef]
16. Mazza, F.; Vulcano, A. Displacement-based design procedure of damped braces for the seismic retrofitting of r.c. framed buildings. *Bull. Earthq. Eng.* **2015**, *13*, 2121–2143. [CrossRef]
17. Ferraioli, M.; Pecorari, O.; Mottola, S.; Diana, A. Dissipative steel exoskeletons for seismic retrofit of RC buildings. *Arch. Civ. Mech. Eng.* **2025**, *25*, 134. [CrossRef]
18. Ferraioli, M.; Pecorari, O.; Diana, A. Dissipative Exoskeletons Based on Self-centering SMA Braces for Seismic Retrofit of RC Buildings. In Proceedings of the International Conference on Protection of Historical Constructions, Naples, Italy, 26–28 March 2025. [CrossRef]
19. Appiied Teehnoiogy Council. *ATC 40 Report—Seismic Evaluation and Retrofit of Concrete Buildings*; Appiied Teehnoiogy Council: Redwood City, CA, USA, 1996.
20. Iervolino, I.; Galasso, C.; Cosenza, E. REXEL: Computer-aided record selection for code-based seismic structural analysis. *Bull. Earthq. Eng.* **2010**, *8*, 339–362. [CrossRef]